https://doi.org/10.5194/egusphere-2025-4014
Preprint. Discussion started: 11 September 2025

Tracking surface ozone responses to clean air interventions under a warming climate in China

Jie Fang[1], Yunjiang Zhang[1*], Didier Hauglustaine[2], Bo Zheng[3], Ming Wang[1], Jingyi Li[1], Yong Sun[4], Haiwei Li[1], Junfeng Wang[1], Yun Wu[1], Mindong Chen[1], Xinlei Ge[5*]

[1]School of Environmental Science and Engineering, Nanjing University of Information Science and Technology, Nanjing 210044, China
[2]Laboratoire des Sciences du Climat et de l'Environnement, CNRS-CEA-UVSQ, Université Paris-Saclay, Gif-sur-Yvette, France
[3]Institute of Environment and Ecology, Tsinghua Shenzhen International Graduate School, Tsinghua University, Shenzhen 518055, China
[4]State Key Laboratory of Tibetan Plateau Earth System, Environment and Resources, Institute of Tibetan Plateau Research, Chinese Academy of Sciences, Beijing 100101, China
[5]School of Energy and Environment, Southeast University, Nanjing 210096, China

Correspondence to: Yunjiang Zhang (yjzhang@nuist.edu.cn) or Xinlei Ge (xinlei@seu.edu.cn)

https://doi.org/10.5194/egusphere-2025-4014
Preprint. Discussion started: 11 September 2025

Abstract. Surface ozone, a major air pollutant with profound implications for human health, ecosystems, and climate, shows long-term trends shaped by both anthropogenic and climatic drivers. Here, we develop a machine learning-based approach – the Fixed Emission Approximation (FEA) – to disentangle the effects of meteorological variability and anthropogenic emissions on summertime ozone trends in China. We identify three distinct phases of ozone trends corresponding to clean air actions. Anthropogenic emissions drove a $+23.2 \pm 1.1$ μg m^{-3} increase in summer maximum daily 8-hour average ozone during 2013–2017, followed by a -4.6 ± 1.5 μg m^{-3} decrease during 2018–2020. However, during 2021–2023, extreme meteorological anomalies – including heatwaves and extended monsoon rainfall – emerged as key drivers of ozone variability. Satellite-derived formaldehyde-to-nitrogen dioxide ratios reveal widespread urban volatile organic compounds-limited regimes, with a shift toward nitrogen oxides-limited sensitivity under influence of heatwaves. Finally, we assess ozone trends under sustained climate warming from 1970 to 2023 based on the FEA framework. The results indicate a significant climate-driven increase in ozone levels across China's urban agglomerations, underscoring the amplifying role of climate change in ozone pollution. Together, these findings highlight the dual influence of anthropogenic and climatic factors on ozone pollution and emphasize the need for integrated strategies that couple emission mitigation with climate adaptation to effectively manage ozone risks in a warming world.

https://doi.org/10.5194/egusphere-2025-4014
Preprint. Discussion started: 11 September 2025

1 Introduction

Surface ozone (O_3) is a critical air pollutant that poses significant threats to human health (Knowlton et al., 2004), ecosystems (Agathokleous et al., 2020), and climate (Fishman et al., 1979; Hauglustaine et al., 1994). It forms through complex photochemical reactions involving nitrogen oxides (NO_x) and volatile organic compounds (VOCs) in the presence of sunlight (Jacob, 2000; Wang et al., 2017) exhibiting a nonlinear response to its precursors (Guo et al., 2023; Liu and Shi, 2021; Wang et al., 2023a). Controlling ozone pollution remains a global environmental challenge. In recent years, China has implemented a series of national clean air actions, most notably the Air Pollution Prevention and Control Action Plan (2013–2017) and the Three-Year Action Plan for Winning the Blue-Sky War (2018–2020) (Geng et al., 2024; Zhang et al., 2019; Zheng et al., 2018), that have markedly improved air quality, particularly by reducing fine particulate matter ($PM_{2.5}$) (Geng et al., 2024; Zhang et al., 2019). However, surface ozone levels have continued to rise in many regions, raising concerns over the complex drivers of ozone trends and highlighting the need for scientific attribution to guide effective mitigation strategies (Li et al., 2019a; Liu et al., 2023; Wang et al., 2023a; Weng et al., 2022).

Long-term ozone variability is jointly influenced by anthropogenic emissions and weather conditions as well as regional climate (Hallquist et al., 2016; Li et al., 2019b; Wang et al., 2022b). While emission controls directly regulate precursor abundance, climate change modulates ozone through chemical feedbacks, meteorological dynamics, and biosphere – atmosphere interactions (Ma and Yin, 2021; Xue et al., 2020). Over the past century, global surface temperatures have increased by approximately 1.2 °C relative to the pre-industrial baseline (1850–1900), driven largely by human activity (Legg, 2021). In a warming world, extreme climate anomalies – such as heatwaves and persistent rainfall shifts – are expected to intensify (Diffenbaugh et al., 2017). These events are increasingly recognized as critical modulators of ozone variability through their impacts on photochemistry, vertical mixing, and precursor transport (Gao et al., 2023; Pu et al., 2017; Wang et al., 2022b).

Quantifying the respective roles of anthropogenic emissions and meteorological variability in driving ozone trends is therefore essential for evaluating the effectiveness of clean air policies (Li et al., 2019a; Liu et al., 2023). Previous studies have reported rapid increases in surface ozone concentrations in key Chinese regions – such as the Beijing–Tianjin–Hebei (BTH) and Yangtze River Delta (YRD) –

https://doi.org/10.5194/egusphere-2025-4014
Preprint. Discussion started: 11 September 2025

during the initial policy phase (2013 – 2017), with increases of approximately 28% and 18%, respectively (Chen et al., 2020; Li et al., 2019a; Liu et al., 2023). In contrast, a modest decline in ozone levels was observed during 2018 – 2020, largely attributed to emission reductions (Li et al., 2021; Liu and Wang, 2020b; Wang et al., 2024b; Wang et al., 2023a). However, since 2021, observations indicate a renewed increase in ozone concentrations (Fig. S1). These fluctuations suggest oscillating trends over the past decade, the drivers of which remain poorly constrained.

Two main approaches have been applied to attribute air pollution trends: chemical transport models (CTMs) (Li et al., 2021; Liu et al., 2023; Liu and Wang, 2020a) and data-driven statistical frameworks (Li et al., 2019a; Li et al., 2019b; Li et al., 2020). CTMs simulate atmospheric composition based on emission inventories, meteorological fields, and chemical mechanisms (Ivatt et al., 2022; Liu and Shi, 2021; Liu et al., 2023; Ye et al., 2024). They allow attribution of trend components to emissions or meteorology, and can resolve sector-specific impacts. However, these models face challenges, including uncertainties and temporal lags in emission inventories. Statistical models, on the other hand, rely on observational datasets and predictor-response relationships without requiring explicit emissions or chemical schemes (Li et al., 2019a; Li et al., 2019b; Li et al., 2020; Zhai et al., 2019). With the growing availability of atmospheric big data, statistical and machine learning models have emerged as powerful tools for trend attribution (Dai et al., 2023; Grange et al., 2018; Vu et al., 2019; Zhang et al., 2025; Zheng et al., 2023). For instance, Grange et al. (2018) developed a random forest-based framework to isolate meteorological influences on particulate matter. Similarly, Wang et al. (2023a) used an enhanced XGBoost model to analyze spatial and temporal ozone patterns in China from 2010 to 2021, confirming that emission reductions played a key role in recent declines. Other recent efforts have extended such models to long-term assessments of air pollution drivers under climate change (Wang et al., 2022c).

Here, we develop a novel machine learning-based framework – Fixed Emission Approximation (FEA) – to quantify the respective roles of anthropogenic emissions and meteorological conditions in shaping summertime surface ozone trends in China. Applying FEA to nationwide observational data from 2013 to 2023, we identify three distinct phases of ozone evolution corresponding to major clean air actions and policy transitions. We further analyze short-term ozone anomalies associated with extreme weather events, such as the 2022 heatwave and seasonal monsoon rainfall. To characterize photochemical regimes, we integrate satellite-derived formaldehyde-to-nitrogen dioxide ($HCHO/NO_2$, FNR) ratios from

https://doi.org/10.5194/egusphere-2025-4014
Preprint. Discussion started: 11 September 2025

Tropospheric Monitoring Instrument (TROPOMI), revealing spatiotemporal shifts in ozone formation sensitivity across China. Finally, we extend our FEA analysis to evaluate climate-driven ozone trends from 1970 to 2023, using historical meteorological reanalysis data. Together, these results provide a comprehensive picture of the anthropogenic and climatic forces shaping surface ozone dynamics in a rapidly warming and urbanizing China.

2 Data and Methods

2.1 Sampling site and instruments

Hourly surface ozone concentration data were obtained from the National Environmental Monitoring Center of China and can be accessed through the open website https://air.cnemc.cn:18007/ (last accessed: May 20, 2024). Hourly meteorological data with a spatial resolution of 0.25° × 0.25° were sourced from the ERA5 reanalysis dataset provided by the European Centre for Medium-Range Weather Forecasts (ECMWF) and are available for download at https://cds.climate.copernicus.eu (last accessed: March 20, 2025). For detailed variables, refer to Table S1. The MDA8 ozone TAP dataset (Geng et al., 2021) for 2013 and 2014 can be downloaded from http://tapdata.org (last accessed: May 20, 2024). The Tropospheric Monitoring Instrument (TROPOMI) on the Sentinel-5P satellite provides global continuous observation data for two indicators of O_3 precursor substances: nitrogen dioxide (NO_2) and formaldehyde (HCHO) concentrations (Lamsal et al., 2014; Shen et al., 2019). The spatial resolution of TROPOMI data is 1113.2 meters (approximately 0.009° in China) (Ren et al., 2022).

2.2 Machine learning-based FEA approach

In this study, we propose a machine learning-based FEA approach to assess the impacts of meteorological factors and anthropogenic emissions on the year-round variations in ozone concentrations. First, we construct a regression model using the random forest (RF) algorithm to relate ozone concentrations to meteorological parameters at various atmospheric heights and to regular emission surrogate parameters (i.e., time variables). The meteorological parameters include 18 distinct variables at different altitudes, while the emission surrogate parameters include the month and the hour of the day, these temporal predictors capture the effects of day-night cycles and workday patterns on air pollutant

https://doi.org/10.5194/egusphere-2025-4014
Preprint. Discussion started: 11 September 2025

concentrations, reflecting the long-term trends in pollutant behavior. The aforementioned variables have been used as typical emission surrogate input features in previous studies (Grange et al., 2018; Meng et al., 2025; Shi et al., 2021; Vu et al., 2019). Our modeling strategy involves building and predicting models for individual cities and for each year from 2015 to 2023. Due to the lack of available observational data for many cities in 2013 and 2014, we did not develop models for these two years. In our approach, 80% of the dataset is used for model training, while the remaining 20% is reserved for testing. We perform ten-fold cross-validation and assess model performance using seven statistical metrics, as listed in Table S2.

Following the construction of the machine learning models for individual cities and years, we introduce the FEA approach. The key principle of FEA is the assumption that the total emissions of ozone precursors remain unchanged from the baseline year. Specifically, using the model trained on data from the baseline year (*i*) as a reference for anthropogenic emissions, we establish hourly-resolution models for the summer months (June to August) of the baseline year. These models are then applied to predict ozone concentrations under the meteorological conditions of the prediction year (*j*), while holding the emission levels constant at those of the baseline year (*i*). The difference between the predicted values and the observed values for the baseline year (*i*) represents the model residuals (RES_i), as shown in Eq. (1). The difference in observed MDA8 ozone concentrations between two different prediction years (j_1, j_2) is driven by the differences in meteorological conditions ($\Delta MET_{i(j1,j2)}$) and anthropogenic emission controls ($\Delta ANT_{i(j1,j2)}$) (Eq. 2). The term $\Delta MET_{i(j1,j2)}$ represents the changes in meteorological conditions and can be calculated by the difference between the predicted values, $Pred_{i(j1)}$ and $Pred_{i(j2)}$, for the corresponding years (Eq. 3). The prediction result $Pred_{i(j)}$ obtained by applying the model trained with data from year *i* to the meteorological conditions of year *j* can be used to calculate the emission-driving variable $ANT_{i(j)}$ corresponding to the model trained in year *i* and the meteorological conditions of year *j* using Eq. (4). Similarly, the value of $\Delta ANT_{i(j1,j2)}$, representing the change in anthropogenic emissions between the two years j_1 and j_2, can be therefore calculated using Eq. (5). By performing these calculations, we can isolate and quantify the contributions of meteorological conditions and anthropogenic emission controls to the observed ozone trends. We used a cross-matrix research method to assess the uncertainty of FEA, with specific formulas available in Supporting Method S1.

https://doi.org/10.5194/egusphere-2025-4014
Preprint. Discussion started: 11 September 2025

$$OBS_i = Pred_i + RES_i\,, \tag{1}$$

$$\Delta OBS_{(j1,j2)} = \Delta MET_{i(j1,j2)} + \Delta ANT_{i(j1,j2)}\,, \tag{2}$$

$$\Delta MET_{i(j1,j2)} = Pred_{i(j2)} - Pred_{i(j1)}\,, \tag{3}$$

$$ANT_{i(j)} = OBS_j - Pred_{i(j)} - RES_i\,, \tag{4}$$

$$\Delta ANT_{i(j1,j2)} = ANT_{i(j2)} - ANT_{i(j1)} = \left(OBS_{j2} - Pred_{i(j2)} - RES_i\right) - \left(OBS_{j1} - Pred_{i(j1)} - RES_i\right)$$

$$= (OBS_{j2} - OBS_{j1}) - (Pred_{i(j2)} - Pred_{i(j1)})\,, \tag{5}$$

Model performance was first evaluated through ten-fold cross-validation for the Beijing–Tianjin–Hebei (BTH) region, revealing high predictive skill between observed and predicted MDA8 ozone levels during 2015-2023 (Fig. S2). The index of agreement (IOA) ranged from 0.96 to 0.97, with correlation coefficients (R) between 0.93 and 0.95. Root mean square errors (RMSE) and normalized mean bias (NMB) varied from 16.9 to 21.9 μg m^{-3} and 8 to 25%, respectively, indicating high model accuracy. Nationally, the model yielded R values of 0.88–0.91 and IOA of 0.93–0.95, with errors remaining within acceptable ranges (Tables S3–S8). To assess uncertainty stemming from interannual model training variability, we applied a matrix-based resampling approach (Supporting Method S1). As shown in Fig. S3, the relative difference in residuals ranged from -9% to 3%, and remained within ±12% for all regions – supporting the robustness of the FEA method.

2.3 Ozone formation regime detection with FNR

Ozone concentrations show a significant nonlinear relationship with their precursors, which can be classified into three types: the VOC-controlled zone, the NO_x-controlled zone, and the excessive/mixed zone. The ratio of HCHO to NO_2 (FNR) serves as a reactive weighting of VOC/NO_x and is one of the diagnostic indicators of ozone-sensitive intervals (Sillman, 1995)， this is particularly suited to the analysis of satellite data and has been widely used in related research (Jin et al., 2020; Jin and Holloway, 2015; Wang et al., 2021).Based on the framework described by Ren et al. (2022) and Jin et al. (2015), we derived a diagnostic approach that is more applicable to our data, and the present study categorizes ozone sensitivity zones for the summer of 2018-2023 according to the following criteria:

$$FNRavg < 4.0\ and\ FNRavg + FNRsd < 6.0: \text{VOC} - \text{controlled zone}$$

$$FNRavg > 4.0\ and\ FNRavg - FNRsd > 2.0: \text{NO}_x - \text{controlled zone}$$

https://doi.org/10.5194/egusphere-2025-4014
Preprint. Discussion started: 11 September 2025

$$Otherwise: excessive/mixed\ zones$$

where $FNRavg$ and $FNRsd$ denote the time-mean and standard deviation of the FNR for the target time period.

2.4 FEA-based assessment of climate change impacts on ozone

To further evaluate the long-term impact of climate change on ozone concentrations over China from 1970 to 2023, we extended the framework of our proposed FEA method. The core idea of this analysis is to isolate the influence of long-term meteorological variations on ozone, assuming fixed anthropogenic emissions. Given the availability of relatively complete and continuous hourly ozone observations and meteorological data across China from 2015 to 2023, we selected this period as the basis for constructing emission baselines.

Following the modeling protocol described in the section Machine learning-based FEA, we trained nine separate random forest models – each using a different year from 2015 to 2023 as an emissions reference. Inputs included hourly ozone observations, key meteorological predictors, and time-related variables (hour of day and month of year). These trained models were then applied to historical reanalysis meteorology from 1970 to 2023 to simulate ozone trends under constant emissions. This yielded nine independent ozone trajectories, each reflecting the influence of long-term meteorological variability under a different fixed-emissions assumption.

While the choice of emission baseline may affect the absolute magnitude of simulated ozone, it does not alter the primary objective: assessing the sensitivity of surface ozone to meteorological drivers over multidecadal timescales (Lecœur et al., 2014; Leung et al., 2018; Wang et al., 2022c). This approach captures the climate-induced ozone signal while adopting the commonly used assumption that emissions are not themselves influenced by climate change – a simplification consistent with prior attribution studies (Dang and Liao, 2019; Leung et al., 2018; Shen et al., 2017; Wang et al., 2022c). For comparison, we also estimated the impact of anthropogenic emission changes on ozone concentrations during the observational window of 2015–2023, using the same FEA methodology and the complete hourly dataset for model training. This dual-track analysis enables a clear distinction between the contributions of climate variability and emission mitigation to observed ozone trends.

https://doi.org/10.5194/egusphere-2025-4014
Preprint. Discussion started: 11 September 2025

3 Results and Discussion

3.1 Spatiotemporal Evolution of Summertime Ozone (2013 – 2023)

Figure 1 presents the interannual variations in maximum daily 8-hour average (MDA8) ozone concentrations during summertime (June–August) across China, with a focus on five key urban agglomerations: Beijing-Tianjin-Hebei (BTH), Yangtze River Delta (YRD), Fenwei Plain (FWP), Sichuan Basin (SCB), and Pearl River Delta (PRD). From 2013 to 2023, summertime ozone levels displayed distinct temporal patterns across regions, reflecting the impact of successive national emission control phases. During the first phase (2013–2017), nationwide MDA8 ozone increased significantly ($p < 0.01$), rising from 95.5 to 118.0 μg m^{-3}. This growth was especially pronounced in the BTH and FWP regions, where concentrations increased by 38% and 41%, respectively. In contrast, ozone increases were more modest in the YRD (11%), SCB (15%), and PRD (16%) regions, respectively. These results were consistent with the previous studies (Li et al., 2021; Liu and Wang, 2020a, b; Wang et al., 2023a).

In the second phase (2017–2020), corresponding to the implementation of more stringent emission controls on NO_x and VOCs emissions (Geng et al., 2024; Liu et al., 2023), a moderate national decrease in MDA8 ozone was observed, with concentrations declining to 109.0 μg m^{-3}. The regional declines during this period were most notable in FWP (−16%) and YRD (−15%), while BTH (−6%), SCB (−11%), and PRD (−4%) also showed reductions compared to their concentration peaks observed in 2017. However, this downward trend did not persist. In the third phase (2020–2023), the MDA8 ozone rebounded, reaching 118.4 μg m^{-3} in 2023 – comparable to its 2017 peak – with a particularly sharp increase during the summer of 2022. From 2021 to 2023, MDA8 ozone concentrations rose by 2.8 μg m^{-3} in BTH, 3.1 μg m^{-3} in FWP, 16.1 μg m^{-3} in YRD, and 18.5 μg m^{-3} in SCB, respectively.

Figure S1 further illustrates the spatiotemporal evolution of summertime MDA8 ozone across 354 cities in China from 2013 to 2023. On average, 68% of cities exceeded the World Health Organization (WHO) air quality guideline of 100.0 μg m^{-3} for the MDA8 ozone. Elevated ozone levels were primarily observed in densely populated and economically developed eastern regions, such as North China Plain. Across the five major city clusters, the average ozone levels ranged from 89.4 to 152.8 μg m^{-3} – substantially exceeding the 43.0 μg m^{-3} threshold associated with ecosystem productivity loss (Gong et al., 2021), implying significant threats to both human and ecological health. Spatially, ozone hotspot

https://doi.org/10.5194/egusphere-2025-4014
Preprint. Discussion started: 11 September 2025

regions expanded between 2013 and 2017 (Fig. S1 a-e), followed by contraction during 2018-2020 (Fig. S1 f-i), reflecting initial policy effectiveness. However, this progress stalled from 2021. A sharp reversal was observed in 2022, with widespread increases in MDA8 ozone (Fig. S1 k), suggesting that the influence of emerging meteorological extremes or evolving ozone photochemical regimes may be counteracting the gains from emission reductions.

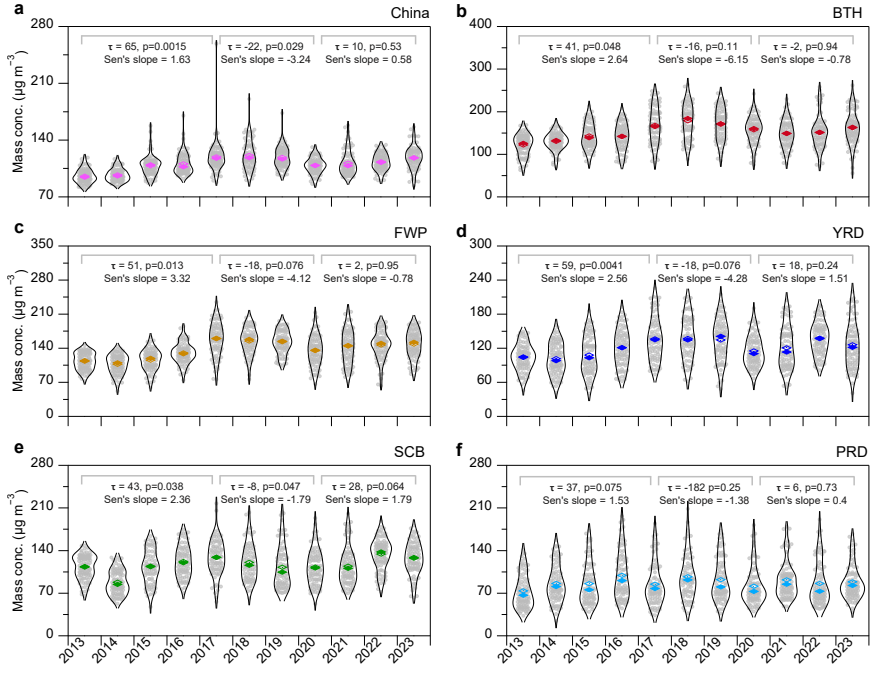

Figure 1. Interannual trends of summertime MDA8 ozone across China (2013–2023). Panel (**a**) illustrate the seasonal variations of MDA8 ozone during the summer months (June, July, and August) across 354 cities nationwide. Panels (**b-f**) shows the average trend across five key regions in China: Beijing-Tianjin-Hebei (BTH), Fenwei Plain (FWP), Yangtze River Delta (YRD), Sichuan Basin (SCB), and Pearl River Delta (PRD). The summer months are defined according to meteorological seasonality, encompassing June, July, and August. In the violin plots, hollow diamond markers denote the mean, while solid diamond markers represent the median. The Mann-Kendall test and Sen's slope estimator were employed to assess the statistical significance and rate of change in the monthly average MDA8 ozone concentrations.

3.2 Anthropogenic drivers of ozone trends

To isolate the influence of anthropogenic emissions on summertime ozone variability, we implemented a machine learning-based FEA framework (Sect. 2.2). This framework employs random forest (RF) models to disentangle the respective contributions of emission changes and meteorological

https://doi.org/10.5194/egusphere-2025-4014
Preprint. Discussion started: 11 September 2025

variability to observed ozone trends. As illustrated in Fig. 2, anthropogenic emissions were the dominant driver of ozone increases during 2013 – 2017, contributing an average rise of 23.2 ± 1.1 μg m^{-3} across 354 cities over China. The strongest regional increases occurred in the FWP and BTH, with contributions of 45.0 ± 2.0 μg m^{-3} and 42.1 ± 2.0 μg m^{-3}, respectively. In contrast, the PRD exhibited a smaller increase (13.4 ± 1.6 μg m^{-3}). These findings indicate that the emission control strategies during China's first phase of air quality control efforts, which primarily focused on reducing $PM_{2.5}$ and haze, inadvertently contributed to worsening ozone pollution by altering the atmospheric chemistry and precursor balance (Zhang et al., 2019; Zheng et al., 2018). This finding is consistent with previous model-based assessments using chemical transport models (Li et al., 2021; Wu et al., 2022), and supports the reliability of the FEA framework in attributing observed ozone changes to underlying drivers.

In 2018, China launched its second-phase Clean Air Action Plan, which aimed to the coordinated control of both $PM_{2.5}$ and ozone by reducing NO_x and VOCs emissions (Zhang et al., 2019; Zheng et al., 2018). During this period (2017-2020), summertime ozone concentrations decreased substantially in northern China. As shown in Fig. 2, the MDA8 ozone declined by 10.5 ± 2.0 μg m^{-3} in BTH and 10.4 ± 3.0 μg m^{-3} in FWP, with smaller but consistent declines in YRD (-4.8 ± 3.8 μg m^{-3}), SCB (-2.8 ± 2.4 μg m^{-3}), and PRD (-6.6 ± 1.4 μg m^{-3}) during 2017 – 2020. These changes underscore the effectiveness of targeted precursor controls and align well with prior studies (Liu et al., 2023; Wang et al., 2023a).

This period also overlapped with the COVID-19 pandemic, which occurred from January to April 2020, introduced an unprecedented, large-scale perturbation to human activity. The nationwide lockdown led to dramatic declines in industrial production, energy consumption, and transportation (Shi and Brasseur, 2020; Zheng et al., 2021). This provided a natural experiment to evaluate the short-term ozone response to abrupt anthropogenic emission reductions. As shown in Fig. S4, from 2017 to 2020, the MDA8 ozone annual mean levels showed a slight national decline, but the pandemic led to an increase in BTH, FWP, YRD, and SCB by +1.7 to +2.3 μg m^{-3}, while PRD experienced a decline. Further analysis (Fig. S5) indicates that ~79% of cities saw increases in ozone during this period, with a national average rise of 2.1 ± 1.3 μg m^{-3}. These increases are consistent with suppressed NO titration and enhanced photochemical ozone production under cleaner atmospheric conditions (Shi et al., 2021; Wang et al., 2022a). In the post-pandemic period (2020–2023), the influence of anthropogenic emissions on

https://doi.org/10.5194/egusphere-2025-4014
Preprint. Discussion started: 11 September 2025

summertime ozone trends became more subdued Emission-driven changes showed relatively small and mixed contributions across all regions, ranging from –1.2 to +2.6 μg m^{-3} in BTH, –1.6 to +4.0 μg m^{-3} in FWP, –4.7 to +7.4 μg m^{-3} in YRD, –3.6 to +3.0 μg m^{-3} in SCB, and –3.8 to +7.7 μg m^{-3} in PRD (Fig. S6). These limited impacts suggest that the benefits of prior emission reduction efforts may have plateaued, and that other drivers – particularly meteorological extremes – are becoming increasingly prominent in shaping ozone variability.

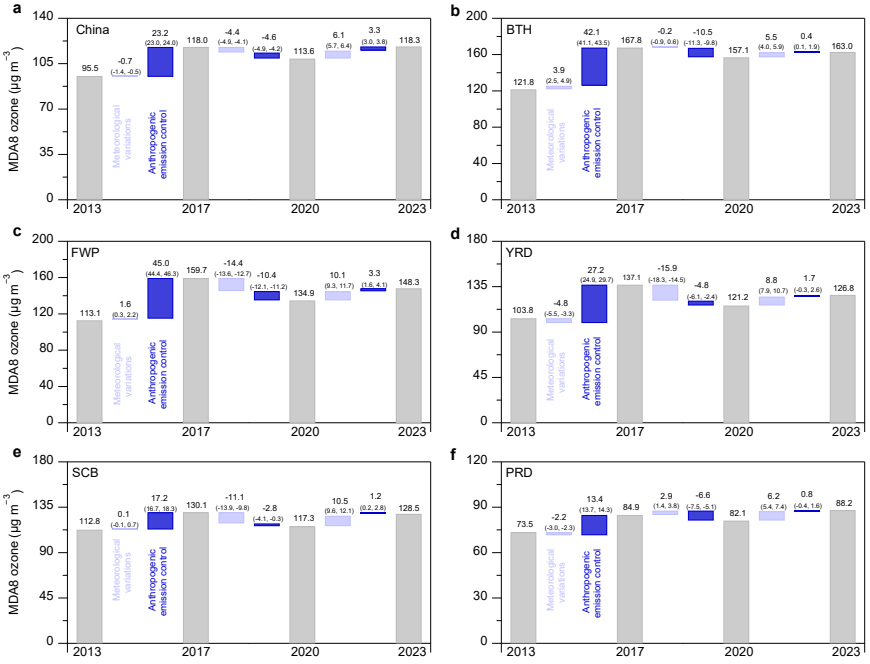

Figure 2. Anthropogenic and meteorological drivers of ozone trends from 2013 to 2023. Changes in summerime MDA8 ozone concentrations were decomposed into contributions from anthropogenic emissions and meteorological variability using the FEA framework. Results reflect ensemble estimates based on multiple baseline years (2015–2023) for emissions. Boxplots indicate the interquartile range, with values in parentheses denoting the 25th and 75th percentiles across all baseline scenarios.

3.3 Ozone formation sensitivity and regime shifts

To diagnose the chemical sensitivity of ozone formation, we analyzed the spatial distributions of tropospheric NO_2 and HCHO columns retrieved by TROPOMI during summer months from 2018 to 2023 (Fig. S7–S8). NO_2 concentrations displayed strong spatial gradients, with eastern China exhibiting levels five times higher than the west – reflecting dense population centers and elevated anthropogenic

https://doi.org/10.5194/egusphere-2025-4014
Preprint. Discussion started: 11 September 2025

NO_x emissions. While NO_2 levels steadily declined over time, the summertime average NO_2 column concentration in the North China Plain decreased from 4.13×10^{15}molecules cm^{-2} in 2018 to 3.85×10^{15} molecules cm^{-2} in 2023, HCHO concentrations remained relatively stable during 2018–2021. However, a sharp increase in HCHO was observed in the Yangtze River Delta during the record-breaking heatwave of 2022, likely due to elevated biogenic and anthropogenic VOC emissions under extreme temperatures (Qin et al., 2025; Tao et al., 2024). By 2023, HCHO levels returned to near-baseline, consistent with cooler summer conditions.

To further characterize the photochemical regimes, we derived the threshold of the $HCHO/NO_2$ ratio (FNR), a widely used proxy for ozone formation sensitivity (Jin and Holloway, 2015; Li et al., 2024; Ren et al., 2022; Wang et al., 2021). As shown in Fig. 3, extensive VOC-limited and transition zones were observed in major megacity clusters. most urbanized regions of China remained within the VOC-limited throughout the study period, with the notable exception of the PRD, which was predominantly NO_x-limited or transitional regimes. This is consistent with previous studies, where VOC-limited regimes primarily appeared in economically developed and densely populated urban areas, with transition zones surrounding VOC-limited areas in large cities and suburbs (Li et al., 2024; Shen et al., 2021).

From 2018 to 2020, regime boundaries exhibited only modest changes. During this period, the VOC-limited areas in the study region gradually decreased, while transition zones correspondingly increased. Additionally, some areas initially classified as transitional regimes shifted to NO_x-limited regimes. The expansion of mixed and NO_x-limited regimes was closely associated with significant NO_x emission reductions (Wang et al., 2023a). In 2021, the VOC-limited area expanded slightly across eastern China. A more dramatic shift occurred in 2022, as extreme heat and elevated VOC levels drove widespread transitions from VOC-limited to transitional or NO_x-limited regimes, especially across the YRD and surrounding regions.

Monthly regime evolution from 2020 to 2023 (Fig. S9) confirms that the most extensive regime shifts occurred in August 2022 (Fig. S9i), coinciding with peak temperatures and FNR anomalies. Notably, VOC-limited areas tended to be smaller in July and August compared to June, likely due to increased VOC reactivity under higher temperatures (Fig. S9). However, major cities generally remained VOC-limited, while adjacent suburban areas shifted dynamically between transitional and VOC-limited regimes. In contrast, outer suburbs and rural regions were more frequently controlled by NO_x (Shen et

https://doi.org/10.5194/egusphere-2025-4014
Preprint. Discussion started: 11 September 2025

al., 2021; Wang et al., 2021). Although VOC-limited regimes partially recovered in 2023, their spatial extent remained smaller than in 2021, likely due to ongoing NO_x emission reductions outpacing changes in VOCs emissions, contributing to a structural shift in ozone formation chemistry. These findings highlight the influence of climate-induced VOCs responses and precursor imbalance in driving ozone formation regime shifts and complicating ozone mitigation efforts. While this influence has already become prominent in the current phase, it is expected to intensify with the increasing frequency of extreme weather events in the future.

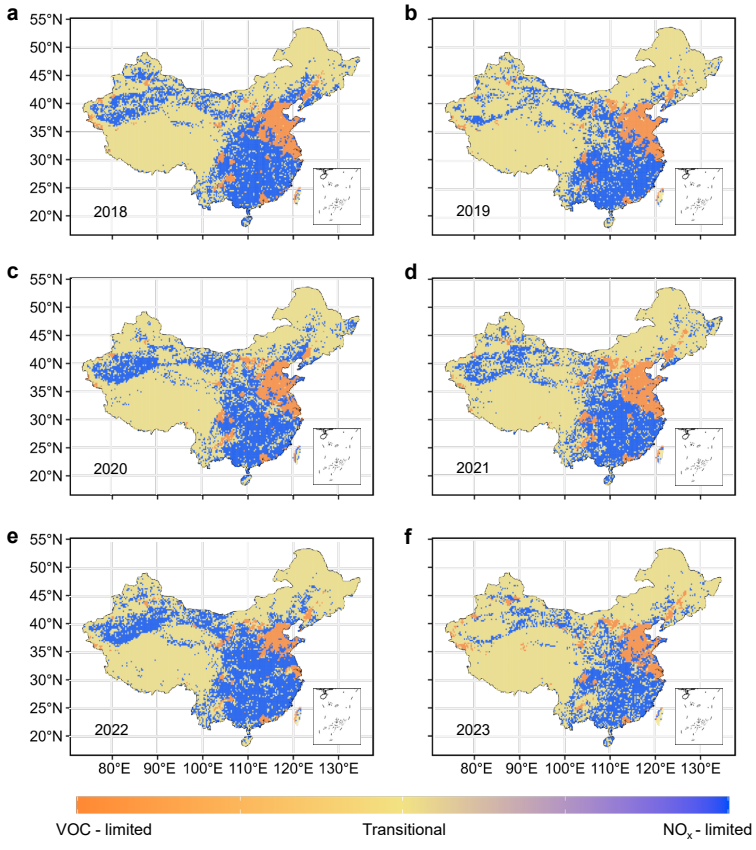

Figure 3. Ozone formation sensitivity regimes. The results of FNR analysis from June to August (2018-2023) are presented, showing the spatiotemporal variation of ozone sensitivity in different regions. The colors in the map represent the geographical distribution of VOC-limited, NO_x-limited, and transitional ozone sensitivity zones. The city locations within the five key regions of China are shown in Fig. S10.

3.4 Impact of meteorological variations on ozone

https://doi.org/10.5194/egusphere-2025-4014
Preprint. Discussion started: 11 September 2025

Meteorological conditions directly and indirectly modulate surface ozone concentrations by influencing photochemical reactions, vertical mixing, and dispersion processes (Li et al., 2019b; Li et al., 2020). These effects exhibit strong regional and temporal heterogeneity across China. As shown in Fig. 2, during Phase I (2013–2017), meteorological contributions to summertime MDA8 ozone remained modest, ranging from -4.8 to +3.9 $\mu g\ m^{-3}$. In Phase II (2017–2020), notable ozone reductions attributable to meteorology were observed – -14.4 ± 3 $\mu g\ m^{-3}$, -15.9 ± 3.8 $\mu g\ m^{-3}$, and -11.1 ± 2.4 $\mu g\ m^{-3}$ in FWP, YRD, and SCB, respectively. These reductions accounted for 58 ± 12%, 77 ± 18%, and 80 ± 17% of the total summertime MDA8 ozone reduction during this phase. however, these impacts remained smaller than those from emission controls in BTH and PRD. In contrast, during 2020–2023, ozone trends became increasingly influenced by meteorological anomalies, particularly in 2022. That summer, extreme heatwaves (Mallapaty, 2022; Wang et al., 2023b) led to sharp increases in MDA8 ozone, contributing 20.8 ± 3.6 $\mu g\ m^{-3}$ in YRD and 22.1 ± 3.2 $\mu g\ m^{-3}$ in SCB. In 2023, however, abundant summer rainfall suppressed ozone formation, with MDA8 ozone decreasing by –17.8 ± 2.3 $\mu g\ m^{-3}$ in YRD and –9.7 ± 3.3 $\mu g\ m^{-3}$ in SCB. These declines correspond to year-on-year increases in rainfall of 102% and 35% in the two regions, respectively (Fig. S11).

To further elucidate the dominant meteorological drivers of ozone variability, we examined Gini importance (Nembrini et al., 2018; Wright and Ziegler, 2017) scores derived from the RF model across 18 predictor variables (Fig. S12). Temperature (*T*) and relative humidity (RH) emerged as the most influential variables in the BTH, FWP, and SCB regions, while in the YRD, shortwave solar radiation (SR), RH, and rainfall were dominant. These results suggest that ozone variability is governed by complex meteorological interactions that vary regionally. For instance, rainfall is typically associated with lower solar irradiance and increased cloud cover, both of which are unfavorable for photochemical ozone production (Jacob and Winner, 2009; Shan et al., 2008). Moreover, the high importance of *T* and SR in these regions indicates that surface ozone is highly sensitive to thermal conditions and photochemical intensity (Yang et al., 2025). Elevated temperatures accelerate ozone precursor emissions and reaction rates, while stronger solar radiation enhances photolysis and ozone formation potential (Qin et al., 2025; Tao et al., 2024). In the PRD, ozone variability was more strongly influenced by temperature and transport-related indices (such as meridional winds at different layers, etc.). This likely reflects the region's subtropical coastal climate, where frequent summer typhoon incursions from the Northwest

https://doi.org/10.5194/egusphere-2025-4014
Preprint. Discussion started: 11 September 2025

Pacific modulate large-scale atmospheric transport (Chen et al., 2024; Wang et al., 2024a; Wang et al., 2022b). These events may introduce strong horizontal advection and vertical mixing, thereby altering the distribution and buildup of ozone precursors, and contributing significantly to the observed ozone variability. As shown in Fig. S13, the correlations between ozone and key meteorological variables were notably enhanced during heatwave (HW) periods. Specifically, ozone positively correlated with both *T* and SR, and negatively (or weakly) correlated with RH. During prolonged rainfall (PR) events, cities in the Yangtze-Huaihe region showed the strongest RH–ozone anti-correlation ($R < -0.7$), likely driven by the enhanced wet scavenging and reduced photochemistry (Fig. S14 a – c).

To quantify the individual contributions of meteorological variables, we applied SHAP (SHapley Additive exPlanations) analysis to HW and PR events in the Yangtze-Huaihe region from 2015 to 2023 (Supporting Methods S3). As shown in Fig. S15 and Fig. S14 d, HW events were associated with strong positive SHAP values in southeastern coastal cities, the YRD, and SCB – primarily driven by elevated SR and *T*. Indeed, mean SR during HW periods was significantly higher than during non-HW periods (Fig. S16), amplifying photochemical ozone production potential. In contrast, PR events consistently yielded negative SHAP contributions across all cities, mainly due to reduced sunlight and suppressed precursor buildup. A multi-year comparison (Fig. 4) highlights the opposing effects of key meteorological variables – including RH, *T*, boundary layer height, total precipitation, and surface pressure – on MDA8 ozone. SR, RH, and *T* emerged as the most influential parameters, while total cloud cover and meteorological transport playing secondary roles during HW episodes. The intensity of HW and PR events modulated the magnitude of these effects. For instance, high-rainfall PR events in 2016 and 2020 yielded large negative SHAP contributions (–29.7 and –16.9 μg m^{-3}), mainly via RH-driven suppression. Conversely, reduced rainfall in 2023 weakened the RH effect, though advection and vertical mixing still contributed to ozone suppression (Fig. S17).

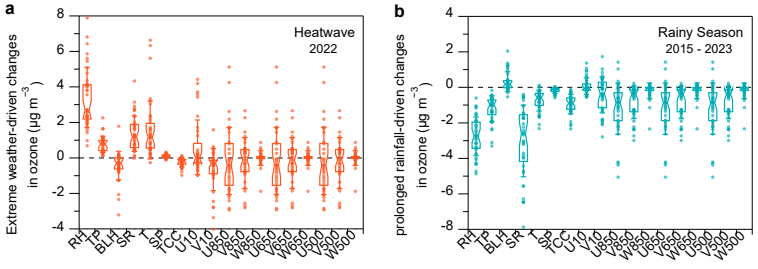

Figure 4. Meteorological influences on predicted ozone concentrations under heatwave and rainy weather conditions. (**a**) Differences in SHAP values (ΔSHAP) between heatwave and non-heatwave periods in the Yangtze-

https://doi.org/10.5194/egusphere-2025-4014
Preprint. Discussion started: 11 September 2025

Huaihe region during summer 2022. (**b**) Differences in SHAP values (ΔSHAP) between prolonged rainfall periods and non-prolonged rainfall periods in the same region from 2015 to 2023. Box plots show the distribution of ΔSHAP across cities; the center line indicates the median, boxes denote the interquartile range (25th-75th percentiles), and whisker line extends to one standard deviation.

3.5 Reshaping ozone trends in a warming climate

To assess the long-term influence of climate change on surface ozone concentrations, we applied the FEA framework to simulate summertime ozone trends over the period 1970 – 2023. In this analysis, anthropogenic emissions were held constant at their 2015 – 2023 summertime levels, while interannual variations in meteorological variables were introduced using historical reanalysis data. This design isolates the climate-driven component of ozone trends while assuming that emission trajectories are independent of climate change – a simplification aligned with prior attribution frameworks (Wang et al., 2022c). The impact of anthropogenic emission controls was estimated by comparing observed ozone concentrations with FEA-predicted values during 2015 – 2023, thereby quantifying the residual effect of emissions under fixed meteorology.

As shown in Fig. 5, under the 2015-2023 emission levels, climate change has exerted a statistically significant ($p < 0.05$) positive influence on urban summertime ozone concentrations across China, resulting in a nationwide increase of approximately 0.06 $\mu g\, m^{-3}\, a^{-1}$ since 1970. All five major urban regions displayed upward trends, with the most pronounced increase observed in the BTH and SCB at 0.12 $\mu g\, m^{-3}\, a^{-1}$. Spatial correlations between climate-driven ozone increases and temperature changes (Fig. S18) further confirm that warming is the dominant contributor to long-term ozone enhancement. In particular, the correlation coefficients between ozone trends and temperature anomalies reached 0.90 (BTH), 0.89 (FWP), 0.72 (YRD), and 0.93 (SCB), indicating a strong temperature dependence of climate-induced ozone formation in these regions. The PRD showed a weaker correlation, likely due to its unique subtropical maritime climate and higher humidity and cloud cover, which tend to suppress photochemical ozone production(Yang et al., 2019).

These findings are consistent with previous projections that forecast an increase in high-ozone events under future climate scenarios spanning 2020–2100 (Li et al., 2023). The historical record already reflects this risk: despite significant increases in anthropogenic emissions driving ozone growth prior to 2018, national air quality improvement measures began to yield reductions thereafter. However, since

https://doi.org/10.5194/egusphere-2025-4014
Preprint. Discussion started: 11 September 2025

2020, a rebound in ozone concentrations has emerged in several regions, suggesting that the climatic penalty for ozone is beginning to offset the benefits of emission control. The intense heatwave of the 2022 summer significantly enhanced ozone formation and altered ozone sensitivity – shifting from a VOC-limited region to a transition zone or NO_x-limited region. Meanwhile, the reduction in anthropogenic emissions of ozone precursor substances indirectly led to changes in ozone sensitivity, thereby making anthropogenic emission reductions more effective in ozone control. However, overall, the direct effects of climate change (i.e., increased ozone formation) far outweigh the indirect effects of anthropogenic emission controls, indicating that the punitive effects of climate change on ozone will become increasingly significant in the future. Taken together, these results underscore the dual challenges of air quality management in a warming climate. Anthropogenic emission reductions remain critical, but they may no longer suffice in isolation. As the warming-driven enhancement of ozone formation becomes more prominent, China and other rapidly urbanizing regions will require adaptive and climate-resilient air quality strategies – including dynamic precursor control, land-use planning, and extreme weather early warning systems –to sustainably mitigate ozone pollution in the decades to come.

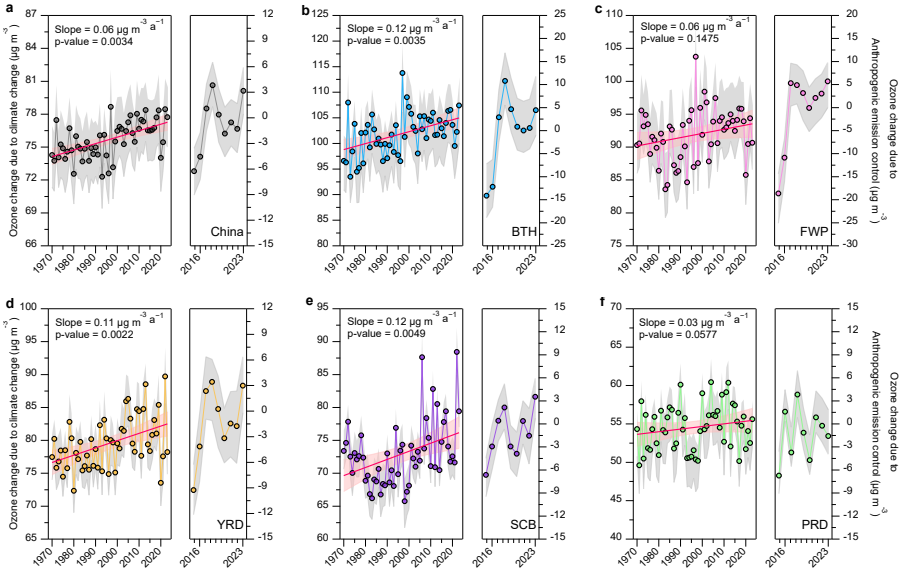

Figure 5. Impact of climate change and emission controls on ozone trends. Left panels show ozone trends attributable to long-term climate change from 1970 to 2023, simulated under fixed emission scenarios using the FEA framework. Right panels depict ozone trends from 2015 to 2023, reflecting the impact of anthropogenic emission controls. Each trajectory represents results based on a distinct emissions baseline year. Shaded grey areas indicate the interquartile range (25th-75th percentiles), solid red lines denote trend estimates, and light red shading marks the

https://doi.org/10.5194/egusphere-2025-4014
Preprint. Discussion started: 11 September 2025

5th-95th percentile confidence intervals. Statistical significance and trend slopes were assessed using the Mann-Kendall test.

4 Conclusions and implications

China is confronted with the dual challenges of climate change and ozone pollution. Over the past decade, summertime ozone concentrations across the country have exhibited complex spatiotemporal patterns, reflecting the evolving interplay between anthropogenic emissions, meteorological variability, and large-scale climate dynamics. In this study, we developed and applied a machine learning-based FEA framework to disentangle and quantify the respective roles of anthropogenic emissions and meteorological drivers in shaping ozone trends during 2013-2023. With a national-level prediction uncertainty of approximately 6%, the FEA method provides a computationally efficient and scalable tool for diagnosing atmospheric variability across large spatial and temporal domains.

Our analysis revealed that increased anthropogenic precursor emissions were the dominant driver of the sharp rise in summertime MDA8 ozone concentrations during the first phase (2013–2017), contributing an average increase of 23.2 ± 1.1 μg m^{-3}. In contrast, during the second phase (2018–2020), enhanced air quality regulations – particularly the synergistic control of NO_x and VOCs – led to measurable reductions in MDA8 ozone, with national-average declines of 4.6 ± 1.5 μg m^{-3}. These improvements were especially evident in regions such as BTH and FWP, where ozone formation is highly sensitive to VOC levels. However, during the most recent period (2021–2023), the impact of emission reductions diminished considerably, with regional ozone levels either plateauing or rebounding. This stagnation underscores the urgent need for more targeted, region-specific emission control strategies that address the shifting photochemical sensitivity of ozone formation regimes.

Applying the SHAP method, we further quantified the impacts of extreme meteorological events on ozone levels. Our results show that record-breaking heatwaves in 2022 contributed to widespread ozone enhancements of up to 5.8 μg m^{-3}, while prolonged rainfall events – particularly during the East Asian plum rain seasons – suppressed ozone production by as much as –15.2 μg m^{-3}.

https://doi.org/10.5194/egusphere-2025-4014
Preprint. Discussion started: 11 September 2025

These findings highlight the increasingly dominant role of short-term meteorological extremes in modulating ozone air quality under a warming climate. In parallel, satellite-based FNR analysis diagnostics revealed that most urban clusters in China remained in VOC-limited or transitional regimes, except the PRD, which was largely NO_x-limited. The 2022 heatwave triggered regime shifts in regions such as the YRD, where rising VOCs emissions and elevated temperatures shifted the photochemical regime toward NO_x-limited. These results emphasize the importance of dynamic, region-specific assessments of ozone formation sensitivity in the formulation of effective mitigation strategies.

To assess the climate penalty on ozone, we extended the FEA framework to simulate long-term trends from 1970 to 2023, by fixing emissions and allowing meteorological variables to evolve with observed climate trends. Our findings show that climate change has contributed a significant upward trend in urban summertime ozone, averaging 0.06 $\mu g\ m^{-3}\ a^{-1}$, with particularly strong increases in the BTH and SCB. Correlations between ozone and surface temperature were consistently high (r = 0.72–0.93) in BTH, FWP, YRD, and SCB, suggesting that warming has increasingly offset gains from emission controls in recent years.

While the FEA framework provides a powerful diagnostic tool, some limitations remain. For example, the historical simulations did not account for climate-driven changes in land use, topography, or population density, which may introduce biases in long-term attribution (Zhu et al., 2025). Future work could incorporate dynamic ancillary datasets and emissions scenarios to further improve model performance. Overall, this study underscores the escalating influence of climate extremes on ozone variability and the emerging limits of conventional emission control approaches. In the face of continued warming, machine learning-based attribution frameworks such as FEA offer a promising pathway for integrating meteorology, chemistry, and policy analysis. To achieve sustained improvements in ozone air quality, future strategies must consider the compound effects of anthropogenic emissions, short-term weather events, and long-term climate change, and adopt adaptive, region-specific, and climate-resilient air quality management frameworks.

https://doi.org/10.5194/egusphere-2025-4014
Preprint. Discussion started: 11 September 2025

Data availability. Data are provided within the manuscript or supplementary information files.

Code availability. The statistical computing in this study was based on R language software which can be download at https://www.r-project.org/.

Author contributions.

Y.Z. and X.G. initiated and designed the study. Y.Z. and JF developed the statistical methodology, model calculation, and data analysis. J.F. and Y.Z. prepared the manuscript with contributions from D.H., B.Z., M.W., J.L., Y.S., H.L., J.W., Y.W., M.C., and X.G..

Competing interests. The authors declare no competing interests.

Acknowledgments.

This study was supported by the National Natural Science Foundation of China (grant no. 42207124) and Natural Science Foundation of Jiangsu Province (grant no. BK20210663).

Correspondence and requests for materials should be addressed to Yunjiang Zhang or Xinlei Ge.

References

Agathokleous, E., Feng, Z., Oksanen, E., Sicard, P., Wang, Q., Saitanis, C.J., Araminiene, V., Blande, J.D., Hayes, F., Calatayud, V., Domingos, M., Veresoglou, S.D., Peñuelas, J., Wardle, D.A., De Marco, A., Li, Z., Harmens, H., Yuan, X., Vitale, M., Paoletti, E.: Ozone affects plant, insect, and soil microbial communities: A threat to terrestrial ecosystems and biodiversity, Sci. Adv., 6, eabc1176, doi: 10.1126/sciadv.abc1176, 2020.

Chen, S., Wang, H., Lu, K., Zeng, L., Hu, M., Zhang, Y.: The trend of surface ozone in Beijing from 2013 to 2019: Indications of the persisting strong atmospheric oxidation capacity, Atmos. Environ., 242, 117801, doi:10.1016/j.atmosenv.2020.117801 , 2020.

Chen, Y., Lu, X., Fung, J.C.H.: Spatiotemporal source apportionment of ozone pollution over the Greater Bay Area, Atmos. Chem. Phys., 24, 8847-8864, doi: 10.5194/acp-24-8847-2024, 2024.

Dai, Q., Dai, T., Hou, L., Li, L., Bi, X., Zhang, Y., Feng, Y.: Quantifying the impacts of emissions and meteorology on the interannual variations of air pollutants in major Chinese cities from 2015 to 2021, Sci. China Earth Sci., 66, 1725-1737, doi: 10.1007/s11430-022-1128-1, 2023.

Dang, R., Liao, H.: Severe winter haze days in the Beijing–Tianjin–Hebei region from 1985 to 2017 and the roles of anthropogenic emissions and meteorology, Atmos. Chem. Phys, 19, 10801-10816, doi:

https://doi.org/10.5194/egusphere-2025-4014
Preprint. Discussion started: 11 September 2025

10.5194/acp-19-10801-2019, 2019.

Diffenbaugh, N.S., Singh, D., Mankin, J.S., Horton, D.E., Swain, D.L., Touma, D., Charland, A., Liu, Y., Haugen, M., Tsiang, M., Rajaratnam, B.: Quantifying the influence of global warming on unprecedented extreme climate events, Proc. Natl. Acad. Sci. USA, 114, 4881-4886, doi: 10.1073/pnas.1618082114, 2017.

Fishman, J., Ramanathan, V., Crutzen, P.J., Liu, S.C.: Tropospheric ozone and climate, Nature, 282, 818-820, doi: 10.1038/282818a0, 1979.

Gao, M., Wang, F., Ding, Y., Wu, Z., Xu, Y., Lu, X., Wang, Z., Carmichael, G.R., McElroy, M.B.: Large-scale climate patterns offer preseasonal hints on the co-occurrence of heat wave and O_3 pollution in China, Proc. Natl. Acad. Sci. USA, 120, e2218274120, doi: 10.1073/pnas.2218274120, 2023.

Geng, G., Liu, Y., Liu, Y., Liu, S., Cheng, J., Yan, L., Wu, N., Hu, H., Tong, D., Zheng, B., Yin, Z., He, K., Zhang, Q.: Efficacy of China's clean air actions to tackle $PM_{2.5}$ pollution between 2013 and 2020, Nat. Geosci., 17, 987-994, doi: 10.1038/s41561-024-01540-z, 2024.

Geng, G., Xiao, Q., Liu, S., Liu, X., Cheng, J., Zheng, Y., Xue, T., Tong, D., Zheng, B., Peng, Y., Huang, X., He, K., Zhang, Q.: Tracking Air Pollution in China: Near Real-Time $PM_{2.5}$ Retrievals from Multisource Data Fusion, Environ. Sci. Technol., 55, 12106-12115, doi: 10.1021/acs.est.1c01863, 2021.

Gong, C., Yue, X., Liao, H., Ma, Y.M.: A humidity-based exposure index representing ozone damage effects on vegetation, Environ. Res. Lett., 16, doi: 10.1088/1748-9326/abecbb, 2021.

Grange, S.K., Carslaw, D.C., Lewis, A.C., Boleti, E., Hueglin, C.: Random forest meteorological normalisation models for Swiss PM_{10} trend analysis, Atmos. Chem. Phys., 18, 6223-6239, doi: 10.5194/acp-18-6223-2018, 2018.

Guo, J., Zhang, X., Gao, Y., Wang, Z., Zhang, M., Xue, W., Herrmann, H., Brasseur, G.P., Wang, T., Wang, Z.: Evolution of Ozone Pollution in China: What Track Will It Follow? Environ. Sci. Technol., 57, 109-117, doi: 10.1021/acs.est.2c08205, 2023.

Hallquist, M., Munthe, J., Hu, M., Wang, T., Chan, C.K., Gao, J., Boman, J., Guo, S., Hallquist, Å.M., Mellqvist, J., Moldanova, J., Pathak, R.K., Pettersson, J.B.C., Pleijel, H., Simpson, D., Thynell, M.: Photochemical smog in China: scientific challenges and implications for air-quality policies. Natl. Sci. Rev., 3, 401-403,doi: 10.1093/nsr/nww080, 2016.

Hauglustaine, D.A., Granier, C., Brasseur, G.P., Mégie, G.: The importance of atmospheric chemistry in the calculation of radiative forcing on the climate system. J. Geophys. Res., 99, 1173-1186, doi: 10.1029/93JD02987, 1994.

Ivatt, P.D., Evans, M.J., Lewis, A.C.: Suppression of surface ozone by an aerosol-inhibited photochemical ozone regime, Nat. Geosci., 15, 536-540, doi: 10.1038/s41561-022-00972-9, 2022.

Jacob, D.J.: Heterogeneous chemistry and tropospheric ozone. Atmos. Environ., 34, 2131-2159, doi: 10.1016/S1352-2310(99)00462-8, 2000.

Jacob, D.J., Winner, D.A.: Effect of climate change on air quality, Atmos. Environ., 43, 51-63, doi: 10.1016/j.atmosenv.2008.09.051, 2009.

Jin, X., Fiore, A., Boersma, K.F., Smedt, I.D., Valin, L.: Inferring changes in cummertime curface czone–NO_x–VOC Chemistry over U.S. urban areas from two decades of satellite and ground-based Observations, Environ. Sci. Technol., 54, 6518-6529, doi: 10.1021/acs.est.9b07785, 2020.

Jin, X., Holloway, T.: Spatial and temporal variability of ozone sensitivity over China observed from the Ozone Monitoring Instrument, J. Geophys. Res. Atmos., 120, 7229-7246, doi: 10.1002/2015JD023250, 2015.

https://doi.org/10.5194/egusphere-2025-4014
Preprint. Discussion started: 11 September 2025

574 Knowlton, K., Rosenthal, J.E., Hogrefe, C., Lynn, B., Gaffin, S., Goldberg, R., Rosenzweig, C., Civerolo,
575 K., Ku, J.-Y., Kinney, P.L.: Assessing Ozone-related health impacts under a changing climate, Environ.
576 Health Perspect., 112, 1557-1563, doi: 10.1289/ehp.716, 2004.
577 Lamsal, L.N., Krotkov, N.A., Celarier, E.A., Swartz, W.H., Pickering, K.E., Bucsela, E.J., Gleason, J.F.,
578 Martin, R.V., Philip, S., Irie, H., Cede, A., Herman, J., Weinheimer, A., Szykman, J.J., Knepp, T.N.:
579 Evaluation of OMI operational standard NO_2 column retrievals using in situ and surface-based NO_2
580 observations, Atmos. Chem. Phys., 14, 11587-11609, doi: 10.5194/acp-14-11587-2014, 2014.
581 Lecœur, È., Seigneur, C., Pagé, C., Terray, L.: A statistical method to estimate $PM_{2.5}$ concentrations from
582 meteorology and its application to the effect of climate change, J. Geophys. Res. Atmos., 119, 3537-
583 3585, doi: 10.1002/2013JD021172, 2014.
584 Legg, S.J.I., 2021. IPCC, 2021: Climate change 2021-the physical science basis, Interaction, 49, 44-45.
585 Leung, D.M., Tai, A.P.K., Mickley, L.J., Moch, J.M., van Donkelaar, A., Shen, L., Martin, R.V.: Synoptic
586 meteorological modes of variability for fine particulate matter ($PM_{2.5}$) air quality in major metropolitan
587 regions of China, Atmos. Chem. Phys., 18, 6733-6748, doi: 10.5194/acp-18-6733-2018, 2018.
588 Li, H., Yang, Y., Jin, J., Wang, H., Li, K., Wang, P., Liao, H.: Climate-driven deterioration of future ozone
589 pollution in Asia predicted by machine learning with multi-source data, Atmos. Chem. Phys., 23, 1131-
590 1145, doi: 10.5194/acp-23-1131-2023, 2023.
591 Li, K., Jacob, D.J., Liao, H., Shen, L., Zhang, Q., Bates, K.H.: Anthropogenic drivers of 2013–2017
592 trends in summer surface ozone in China, Proc. Natl. Acad. Sci. USA, 116, 422-427, doi:
593 10.1073/pnas,1812168116, 2019a.
594 Li, K., Jacob, D.J., Liao, H., Zhu, J., Shah, V., Shen, L., Bates, K.H., Zhang, Q., Zhai, S.: A two-pollutant
595 strategy for improving ozone and particulate air quality in China. Nat. Geosci., 12, 906-910, doi:
596 10.1038/s41561-019-0464-x, 2019b.
597 Li, K., Jacob, D.J., Shen, L., Lu, X., De Smedt, I., Liao, H.: Increases in surface ozone pollution in China
598 from 2013 to 2019: anthropogenic and meteorological influences, Atmos. Chem. Phys., 20, 11423-
599 11433, doi: 10.5194/acp-20-11423-2020, 2020.
600 Li, M., Wang, T., Shu, L., Qu, Y., Xie, M., Liu, J., Wu, H., Kalsoom, U.: Rising surface ozone in China
601 from 2013 to 2017: A response to the recent atmospheric warming or pollutant controls? Atmos.
602 Environ., 246, 118130,doi: 10.1016/j.atmosenv.2020.118130, 2021.
603 Li, Y., Yu, C., Tao, J., Lu, X., Chen, L.: Analysis of ozone formation Sensitivity in Chinese representative
604 regions using satellite and ground-based Data, Remote Sens., 16, 316, doi: 10.3390/rs16020316, 2024.
605 Liu, C., Shi, K.: A review on methodology in O_3-NO_x-VOC sensitivity study, Environ. Pollut., 291,
606 118249, doi: 10.1016/j.envpol.2021.118249, 2021.
607 Liu, Y., Geng, G., Cheng, J., Liu, Y., Xiao, Q., Liu, L., Shi, Q., Tong, D., He, K., Zhang, Q.: Drivers of
608 increasing ozone during the two phases of clean air actions in China 2013–2020, Environ. Sci. Technol.,
609 57, 8954-8964, doi: 10.1021/acs.est.3c00054, 2023.
610 Liu, Y., Wang, T. Worsening urban ozone pollution in China from 2013 to 2017 – Part 1: The complex
611 and varying roles of meteorology, Atmos. Chem. Phys., 20, 6305-6321,doi: 10.5194/acp-20-6305-
612 2020, 2020a.
613 Liu, Y., Wang, T.: Worsening urban ozone pollution in China from 2013 to 2017 – Part 2: The effects of
614 emission changes and implications for multi-pollutant control, Atmos. Chem. Phys., 20, 6323-6337,
615 doi: 10.5194/acp-20-6323-2020, 2020b.
616 Ma, X., Yin, Z.: Dipole pattern of summer ozone pollution in the east of China and its connection with
617 climate variability, Atmos. Chem. Phys., 21, 16349-16361, doi: 10.5194/acp-21-16349-2021, 2021.

https://doi.org/10.5194/egusphere-2025-4014
Preprint. Discussion started: 11 September 2025

618 Mallapaty, S.: China's extreme weather challenges scientists trying to study it, Nature, 609, 888-888, doi:
619 10.1038/d41586-022-02954-8, 2022.
620 Meng, Q., Zhang, Y., Zhong, S., Fang, J., Tang, L., Rao, Y., Zhou, M., Qiu, J., Xu, X., Petit, J.-E.J.A.C.,
621 Physics: Reconstructing missing surface aerosol elemental carbon data in long-term series with
622 ensemble learning. Atmos. Chem. Phys., 25, 7485-7498, doi: 10.5194/acp-25-7485-2025, 2025.
623 Nembrini, S., König, I.R., Wright, M.N.J.B. The revival of the Gini importance? Bioinformatics, 34,
624 3711-3718, doi: 10.1093/bioinformatics/bty373, 2018.
625 Pu, X., Wang, T.J., Huang, X., Melas, D., Zanis, P., Papanastasiou, D.K., Poupkou, A.: Enhanced surface
626 ozone during the heat wave of 2013 in Yangtze River Delta region, China, Sci. Total Environ., 603-
627 604, 807-816, doi: 10.1016/j.scitotenv.2017.03.056, 2017.
628 Qin, M., She, Y., Wang, M., Wang, H., Chang, Y., Tan, Z., An, J., Huang, J., Yuan, Z., Lu, J., Wang, Q.,
629 Liu, C., Liu, Z., Xie, X., Li, J., Liao, H., Pye, H.O.T., Huang, C., Guo, S., Hu, M., Zhang, Y., Jacob,
630 D.J., Hu, J.: Increased urban ozone in heatwaves due to temperature-induced emissions of
631 anthropogenic volatile organic compounds, Nat. Geosci, 18, 50-56, doi: 10.1038/s41561-024-01608-
632 w, 2025.
633 Ren, J., Guo, F., Xie, S.: Diagnosing ozone–NO_x–VOC sensitivity and revealing causes of ozone
634 increases in China based on 2013–2021 satellite retrievals, Atmos. Chem. Phys., 22, 15035-15047, doi:
635 10.5194/acp-22-15035-2022, 2022.
636 Shan, W., Yin, Y., Zhang, J., Ding, Y.: Observational study of surface ozone at an urban site in East China,
637 Atmos. Res., 89, 252-261, doi: 10.1016/j.atmosres.2008.02.014, 2008.
638 Shen, H., Sun, Z., Chen, Y., Russell, A.G., Hu, Y., Odman, M.T., Qian, Y., Archibald, A.T., Tao, S.: Novel
639 method for ozone isopleth construction and diagnosis for the ozone control strategy of Chinese cities,
640 Environ. Sci. Technol., 55, 15625-15636, doi: 10.1021/acs.est.1c01567, 2021.
641 Shen, L., Jacob, D.J., Zhu, L., Zhang, Q., Zheng, B., Sulprizio, M.P., Li, K., De Smedt, I., González Abad,
642 G., Cao, H., Fu, T.-M., Liao, H.: The 2005–2016 trends of formaldehyde columns over China observed
643 by satellites: increasing anthropogenic emissions of volatile organic compounds and decreasing
644 agricultural fire emissions, Geophys. Res. Lett., 46, 4468-4475,doi: 10.1029/2019GL082172, 2019.
645 Shen, L., Mickley, L.J., Murray, L.T.: Influence of 2000–2050 climate change on particulate matter in
646 the United States: results from a new statistical model, Atmos. Chem. Phys., 17, 4355-4367, doi:
647 10.5194/acp-17-4355-2017, 2017.
648 Shi, X., Brasseur, G.P.: The response in air quality to the reduction of Chinese economic activities during
649 the COVID-19 outbreak, Geophys. Res. Lett., 47, e2020GL088070, doi: 10.1029/2020GL088070,
650 2020.
651 Shi, Z., Song, C., Liu, B., Lu, G., Xu, J., Van Vu, T., Elliott, R.J.R., Li, W., Bloss, W.J., Harrison, R.M.:
652 Abrupt but smaller than expected changes in surface air quality attributable to COVID-19 lockdowns,
653 Sci. Adv., 7, eabd6696, doi: 10.1126/sciadv.abd6696, 2021.
654 Sillman, S.: The use of NO_y, H_2O_2, and HNO_3 as indicators for ozone-NO_x-hydrocarbon sensitivity in
655 urban locations, J. Geophys. Res., 100, 14175-14188, doi: 10.1029/94JD02953, 1995.
656 Tao, C., Zhang, Y., Zhang, X., Guan, X., Peng, Y., Wang, G., Zhang, Q., Ren, Y., Zhao, X., Zhao, R.,
657 Wang, Q., Wang, W.: Discrepant global surface ozone responses to emission- and heatwave-induced
658 regime shifts, Environ. Sci. Technol., 58, 22288-22297, doi: 10.1021/acs.est.4c08422, 2024.
659 Vu, T.V., Shi, Z., Cheng, J., Zhang, Q., He, K., Wang, S., Harrison, R.M.: Assessing the impact of clean
660 air action on air quality trends in Beijing using a machine learning technique, Atmos. Chem. Phys., 19,
661 11303-11314, doi: 10.5194/acp-19-11303-2019, 2019.

https://doi.org/10.5194/egusphere-2025-4014
Preprint. Discussion started: 11 September 2025

Wang, H., Huang, C., Tao, W., Gao, Y., Wang, S., Jing, S., Wang, W., Yan, R., Wang, Q., An, J., Tian, J., Hu, Q., Lou, S., Pöschl, U., Cheng, Y., Su, H.: Seasonality and reduced nitric oxide titration dominated ozone increase during COVID-19 lockdown in eastern China, npj Clim. Atmos. Sci., 5, 24, doi: 10.1038/s41612-022-00249-3, 2022a.

Wang, J., Wang, P., Tian, C., Gao, M., Cheng, T., Mei, W.: Consecutive Northward Super Typhoons Induced Extreme Ozone Pollution Events in Eastern China, npj Clim. Atmos. Sci., 7, 244,doi: 10.1038/s41612-024-00786-z, 2024a.

Wang, M., Chen, X., Jiang, Z., He, T.-L., Jones, D., Liu, J., Shen, Y.: Meteorological and anthropogenic drivers of surface ozone change in the North China Plain in 2015–2021, Sci. Total Environ., 906, 167763, doi: 10.1016/j.scitotenv.2023.167763, 2024b.

Wang, N., Huang, X., Xu, J., Wang, T., Tan, Z.-m., Ding, A.: Typhoon-boosted biogenic emission aggravates cross-regional ozone pollution in China, Sci. Adv., 8, eabl6166, doi: 10.1126/sciadv.abl6166, 2022b.

Wang, R., Yang, Y., Xing, X., Wang, L., Chen, J., Tang, X., Cao, J., Morawska, L., Balkanski, Y., Hauglustaine, D., Ciais, P., Ma, J.: Stringent emission controls are needed to reach clean air targets for cities in China under a warming climate, Environ. Sci. Technol., 56, 11199-11211, doi: 10.1021/acs.est.1c08403, 2022c.

Wang, T., Xue, L., Brimblecombe, P., Lam, Y.F., Li, L., Zhang, L.: Ozone pollution in China: A review of concentrations, meteorological influences, chemical precursors, and effects, Sci. Total Environ., 575, 1582-1596, doi: 10.1016/j.scitotenv.2016.10.081, 2017.

Wang, W., van der A, R., Ding, J., van Weele, M., Cheng, T.: Spatial and temporal changes of the ozone sensitivity in China based on satellite and ground-based observations, Atmos. Chem. Phys., 21, 7253-7269, doi: 10.5194/acp-21-7253-2021, 2021.

Wang, Y., Zhao, Y., Liu, Y., Jiang, Y., Zheng, B., Xing, J., Liu, Y., Wang, S., Nielsen, C.P.: Sustained emission reductions have restrained the ozone pollution over China, Nat. Geosci., 16, 967-974, doi: 10.1038/s41561-023-01284-2, 2023a.

Wang, Z.Q., Luo, H.L., Yang, S.: Different mechanisms for the extremely hot central-eastern China in July-August 2022 from a Eurasian large-scale circulation perspective, Environ. Res. Lett. 18,doi: 10.1088/1748-9326/acb3e5, 2023b.

Weng, X., Forster, G.L., Nowack, P.: A machine learning approach to quantify meteorological drivers of ozone pollution in China from 2015 to 2019, Atmos. Chem. Phys., 22, 8385-8402, doi: 10.5194/acp-22-8385-2022, 2022.

Wright, M.N., Ziegler, A.J.J.o.s.s. ranger: A fast implementation of random forests for high dimensional data in C++ and R. J. Stat. Soft., 77, 1-17, ndoi: 10.18637/jss.v077.i01, 2017.

Wu, K., Wang, Y., Qiao, Y., Liu, Y., Wang, S., Yang, X., Wang, H., Lu, Y., Zhang, X., Lei, Y.: Drivers of 2013–2020 ozone trends in the Sichuan Basin, China: Impacts of meteorology and precursor emission changes, Environ. Pollut., 300, 118914, doi: 10.1016/j.envpol.2022.118914, 2022.

Xue, L., Ding, A., Cooper, O., Huang, X., Wang, W., Zhou, D., Wu, Z., McClure-Begley, A., Petropavlovskikh, I., Andreae, M.O., Fu, C.: ENSO and Southeast Asian biomass burning modulate subtropical trans-Pacific ozone transport, Natl. Sci. Rev., 8, doi: 10.1093/nsr/nwaa132, 2020.

Yang, J., Wang, Y., Zhang, L., Zhao, Y.: Investigating the response of China's surface ozone concentration to the future changes of multiple factors, Atmos. Chem. Phys, 25, 2649-2666, doi: 10.5194/acp-25-2649-2025, 2025.

Yang, L., Luo, H., Yuan, Z., Zheng, J., Huang, Z., Li, C., Lin, X., Louie, P.K.K., Chen, D., Bian, Y.:

https://doi.org/10.5194/egusphere-2025-4014
Preprint. Discussion started: 11 September 2025

Quantitative impacts of meteorology and precursor emission changes on the long-term trend of ambient ozone over the Pearl River Delta, China, and implications for ozone control strategy, Atmos. Chem. Phys., 19, 12901-12916, doi: 10.5194/acp-19-12901-2019, 2019.

Ye, X., Zhang, L., Wang, X., Lu, X., Jiang, Z., Lu, N., Li, D., Xu, J. Spatial and temporal variations of surface background ozone in China analyzed with the grid-stretching capability of GEOS-Chem High Performance. Sci. Total Environ., 914, 169909,doi: 10.1016/j.scitotenv.2024.169909, 2024.

Zhai, S., Jacob, D.J., Wang, X., Shen, L., Li, K., Zhang, Y., Gui, K., Zhao, T., Liao, H.: Fine particulate matter ($PM_{2.5}$) trends in China, 2013–2018: separating contributions from anthropogenic emissions and meteorology, Atmos. Chem. Phys., 19, 11031-11041, doi: 10.5194/acp-19-11031-2019, 2019.

Zhang, Q., Zheng, Y., Tong, D., Shao, M., Wang, S., Zhang, Y., Xu, X., Wang, J., He, H., Liu, W., Ding, Y., Lei, Y., Li, J., Wang, Z., Zhang, X., Wang, Y., Cheng, J., Liu, Y., Shi, Q., Yan, L., Geng, G., Hong, C., Li, M., Liu, F., Zheng, B., Cao, J., Ding, A., Gao, J., Fu, Q., Huo, J., Liu, B., Liu, Z., Yang, F., He, K., Hao, J.: Drivers of improved $PM_{2.5}$ air quality in China from 2013 to 2017, Proc. Natl. Acad. Sci. USA, 116, 24463-24469,doi: 10.1073/pnas.1907956116, 2019.

Zhang, Y., Li, N., Tang, K., Wang, M., Li, H., Li, K., Zheng, B., Zhang, Q., Gao, M., Fang, J.J.S.A.: Widespread surface ozone reduction triggered by dust storm disturbance on ozone production and destruction chemistry. Sci. Adv., 11, eadr4297, doi: 10.1126/sciadv.adr4297, 2025.

Zheng, B., Tong, D., Li, M., Liu, F., Hong, C., Geng, G., Li, H., Li, X., Peng, L., Qi, J., Yan, L., Zhang, Y., Zhao, H., Zheng, Y., He, K., Zhang, Q.: Trends in China's anthropogenic emissions since 2010 as the consequence of clean air actions, Atmos. Chem. Phys., 18, 14095-14111,doi: 10.5194/acp-18-14095-2018, 2018.

Zheng, B., Zhang, Q., Geng, G., Chen, C., Shi, Q., Cui, M., Lei, Y., He, K.: Changes in China's anthropogenic emissions and air quality during the COVID-19 pandemic in 2020, Earth Syst. Sci. Data, 13, 2895-2907, doi: 10.5194/essd-13-2895-2021, 2021.

Zheng, H., Kong, S., Zhai, S., Sun, X., Cheng, Y., Yao, L., Song, C., Zheng, Z., Shi, Z., Harrison, R.M.: An intercomparison of weather normalization of $PM_{2.5}$ concentration using traditional statistical methods, machine learning, and chemistry transport models, npj Clim. Atmos. Sci., 6, 214, doi: 10.1038/s41612-023-00536-7, 2023.

Zhu, J., Penner, J.E., Hong, C., Liu, H., Zhao, X., Deng, J., Liu, C.-Q., Zhang, Q., Fu, P.: Cropland expansion reduces biogenic secondary organic aerosol and associated radiative cooling, Nat. Geosci., 18, 624-630, doi: 10.1038/s41561-025-01718-z, 2025.